IODA: A Host/Device Co-Design for Strong Predictability Contract on Modern Flash Storage

Huaicheng Li
University of Chicago and
Carnegie Mellon University

Martin L. Putra
University of Chicago

Ronald Shi
University of Chicago

Xing Lin
NetApp

Gregory R. Ganger
Carnegie Mellon University

Haryadi S. Gunawi
University of Chicago

Abstract

Predictable latency on flash storage is a long-pursuit goal, yet, unpredictability stays due to the unavoidable disturbance from many well-known SSD internal activities. To combat this issue, the recent NVMe IO Determinism (IOD) interface advocates host-level controls to SSD internal management tasks. While promising, challenges remain on how to exploit it for truly predictable performance.

We present IODA, *an I/O deterministic flash array design built on top of small but powerful extensions to the IOD interface for easy deployment.* IODA *exploits data redundancy in the context of IOD for a strong latency predictability contract. In* IODA, *SSDs are expected to quickly fail an I/O on purpose to allow predictable I/Os through proactive data reconstruction. In the case of concurrent internal operations,* IODA *introduces busy remaining time exposure and predictable-latency-window formulation to guarantee predictable data reconstructions. Overall,* IODA *only adds 5 new fields to the NVMe interface and a small modification in the flash firmware, while keeping most of the complexity in the host OS. Our evaluation shows that* IODA *improves the 95–99.99th latencies by up to 75×.* IODA *is also the nearest to the ideal, no disturbance case compared to 7 state-of-the-art preemption, suspension, GC coordination, partitioning, tiny-tail flash controller, prediction, and proactive approaches.*

CCS Concepts

• **Computer systems organization** → **Firmware**; **Embedded hardware**; **Embedded software**; • **Information systems** → **Flash memory**; • **Hardware** → **Emerging interfaces**.

Keywords

Software/Hardware Co-Design, Predictable Latency, NVMe I/O Determinism, SSD, Flash Storage

1 Introduction

Flash arrays are popular storage choices in data centers and they must address users' craving for low and predictable latencies [1–3]. Thus, many recent SSD products are released and evaluated not just on the average speed but the percentile latencies as well [4–7]. These all paint the reality that customers would like SSDs with *deterministic* latencies.

Deterministic latency, however, is hard to achieve because SSD performance is inherently non-deterministic due to the internal management activities such as the garbage collection (GC) process, wear leveling, and internal buffer flush [8–10]. These activities will inevitably trigger many background I/Os and disturb user requests. Notably, GC is a necessary path to overcome NAND Flash's inability for in-place overwrites. It involves time-consuming data movement to reclaim space and contend with user requests, thereby causing severe latency hiccups. As an illustration, the figure on the right shows the giant latency gap between the "Base" (with GC) and the "Ideal" (no GC) cases. Modern SSDs often resort to large over-provisioning space (*e.g.*, up to 50% of the SSD's raw NAND capacity) [11] to provide legroom for more efficient background task processing, however, our profiling experiments on recent enterprise SSDs showed that GCs can still cause up to 60× latency increase (details omitted). This is unfortunately still an ongoing problem faced by the storage industry [12–14].

To tame the SSD performance challenges, there have been many efforts to evolve the device interfaces [15–17]. The Stor-

age Interface Technical Committee has standardized many extensions over the last decade: from `UNMAP/TRIM` (2011) [15], `ATOMIC_WRITE` (2013) [16], `STREAM` (2017) [17], to a recent one, the NVMe I/O Determinism (**IOD**) interface (2019) [18]. One IOD feature is the *predictable latency mode* (**PLM**) interface, which suggests SSDs work in two alternating modes across time: the deterministic (predictable) and non-deterministic ("busy" for short). IOD-PLM tries to deliver the best I/O latency during the predictable mode and only schedules background activities in the busy mode. The specification does not provide the exact definition of "deterministic window," but a common understanding suggests that in a deterministic window, the device should **not** perform internal activities that would cause unpredictable latencies to user I/Os. (*i.e.*, background operations should only be done in the busy window). IOD-PLM is a major leap towards a more open host-SSD collaboration in attacking the latency consistency challenge. However, it is still considered a "young" interface. Challenges remain on how the host OS and SSDs should be co-designed around this interface.
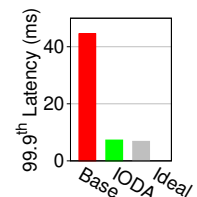
IOD-PLM is expected to be useful for flash arrays or clusters where the host or applications can redirect I/Os to devices in the deterministic mode, whenever possible. Let's take the read operation on a RAID-5 flash array as an example. Here, an "**unpredictable I/O**" destined to a busy device can be **reconstructed** using the parity and the rest of the data blocks in the same stripe. The reconstruction is done by the "**array's host**" (*e.g.*, software/hardware array controller). Suppose a stripe consists of 3 data chunks (B_0, B_1, B_2) and 1 parity chunk (P), if reading B_0 is unpredictable because device #0 is busy, B_0 can be reconstructed by reading the parity and other chunks within the stripe ($B_0=B_1 \oplus B_2 \oplus P$), with the hope that other devices (#1 to #3) are in the deterministic state. This proactive reconstruction scheme is often referred to as "degraded reads" [9, 19–22], a popular concept used when parity computation is much faster than waiting.

While degraded-reads seem to be straightforward and a natural fit for IOD-PLM, we discovered a number of shortcomings (detailed later) during our journey to exploit the interface for an always-deterministic flash array design. To this end, we introduce **IODA**[1], an I/O deterministic flash array built on top of small but powerful extensions to the IOD-PLM interface.

IODA introduces three main techniques to enhance the IOD interface and facilitate a deterministic host/SSD co-design incorporating degraded-reads seamlessly: **(1)** predictable mode I/Os for augmenting coarse-grained whole-device level predictability with per-I/O level predictability query via a simple flag ("Will this I/O be predictable? Yes/No"); This allows a more live response of the predictability status to signal the host decisively on whether and when to trigger reconstructions. **(2)** piggybacking busy remaining time

---

for assisting the host in picking less-busy devices for reconstructions in the case of concurrent internal operations. Thus, we only need to wait for the least busy devices to achieve improved latencies; and **(3)** a stronger (un)predictable-latency-window formulation and scheduling scheme for programming a proper upper bound value of the (un)predictable window in every device of the array to guarantee a stronger predictability contract. We show how the combination of these approaches is more powerful than each of the individual methods. Our techniques add only 5 new fields to the existing IOD-PLM interface and NVMe commands (18 lines in the Linux NVMe driver), keep the flash firmware simple (only 60 and 186 lines of new logic on 2 popular SSD platforms [23, 24], respectively), and isolate all the complexity in the host OS, with 1814 new lines in the Linux RAID ("`md`") sub-system.

We performed a thorough evaluation (§5) with 9 datacenter I/O traces, 6 file system, and 15 popular data-intensive workloads. Compared to the baseline, IODA reduces I/O latency by 1–75× between p95–p99.99 (*i.e.*, the 95–99.99th percentiles) and 1.7–16.3× on average. Compared to an "ideal" scenario where there are no write-triggered GCs, IODA is only 1.0–3.3× slower between p95–p99.99 while the baseline suffers from 1.1–88.3× degradation. To compare IODA with state-of-the-art approaches, we also re-implement 7 published methods that represent preemption [25–27], program/erase suspension [28–30], speculation [31, 32], GC coordination [33, 34], partitioning [35–37], "tiny-tail" controller design [9], and SLO-aware prediction [38].

Overall, our measurements show that IODA provides a strong IOD guarantee (no I/Os delayed by GCs), even under the maximum write burst, and without sacrificing throughput; to the best of our knowledge the *first* flash array design that has achieved so. For the rest of the paper, we assume flash arrays with some level of redundancy. We use N_{ssd} and k to represent the number of devices and parities (*e.g.*, N_{ssd}=4 and k=1 in a 4-drive RAID-5 array).

2 IOD-PLM: The Good and The Better

2.1 How IOD-PLM Works

The NVMe I/O Determinism (IOD) concept [18] introduces two interfaces: "NVM Set" (for isolation, not our focus) and predictable latency mode (**PLM**). PLM suggests SSDs work in two alternating modes across time: **deterministic (predictable)** and **non-deterministic ("busy") windows**. A common understanding suggests that background operations should only be done in the busy window. In more detail, PLM exposes two NVMe commands. First, the "`GetPLMLogPage`" command ("`PLM-Query`" for short) allows the **host OS** (*e.g.*, Linux RAID) to query the device state such as the #I/Os in the future that the device can guarantee to be deterministic in latency. Second, the "`PLM-Config`" command allows the host to toggle the device's deterministic/busy state. *However*, one caveat is that this IOD interface is seen as a "best-effort, soft

---

[1]IODA is pronounced "**Yoda**," a wise and determined Jedi Master

contract," *i.e.*, the device can autonomously transit to the busy state under certain conditions (*e.g.*, performing GCs when running out of over-provisioning space), hence breaking the predictability guarantee.

2.2 Opportunities for Improvement

PLM is a major leap towards more open host-SSD communication and the interface keeps evolving. We argue it requires further enhancement to enable a principled co-design for strong predictability due to the following deficiencies.

First, `PLM-Query` returns significant information of the device PLM state [18, §8.18] without (so far) much guidance on how the host should use them. Both the host and the device must keep track of this "soft contract," (*e.g.*, extensive inflight I/O status) which can create much management complexities.

Second, the whole-device non-deterministic mode is unnecessarily too coarse-grained. Modern SSDs have many parallel channels (*e.g.*, 16 or more) where a GC activity on certain channels will not disturb user requests on other channels. However, because the device declares to be busy as a whole, the host might unnecessarily reconstruct I/Os from other devices while the I/Os could have been destined to non-busy channels inside the currently busy device. This limitation would adversely increase overall system resource utilization and jeopardize performance predictability.

Third, the PLM busy window duration is vital for a strong predictability guarantee (more in §3.3), however, we are not aware of any work that attempts to analyze and formulize the proper window size. In particular, we need a "configurable" framework to lay out how these values are derived and program them properly. The PLM's "soft" control of the busy/predictable window transition is far from being ideal.

2.3 Related Work and Our Contributions

Table 1 summarizes existing approaches that attack the flash performance challenges. The popular methods include preemptions [25, 28, 39], hints [38, 40–43], partitioning [10, 36, 37, 44], speculation [21, 45, 46], latency prediction [38, 47], and coordinated GCs [9, 33–35, 48, 49]. Traditional preemptions cannot indefinitely avoid/postpone GCs, as they will revert to normal blocking behavior under insufficient over-provisioning space. Hint-schemes such as [43] require code changes, breaking application transparency. Partitioning methods like FlashBlox [36] exploit parallel hardware resources (channels/chips) to achieve strong isolation at the cost of the aggregate bandwidth drop. I/O speculation techniques, *e.g.*, request cloning or hedging [2] pose the question of *how long* to wait before forcing an I/O reconstruction/replication; it remains challenging to adapt the speculation eagerness for balanced resource utilization and effectiveness. Latency prediction approaches such as MittOS [38] or LinnOS [47] answer the *when*-to-reconstruct question but suffer from inaccuracies without collaboration with the device. Coordinated GCs, as in TTFLASH [9], overcome latency prediction limi-

	IODA	Preemption	Partitioning	Speculation	Suspension	Coordination	TTFLASH	Prediction
Determinism	✓	✗	✓	✗	✗	✗	✓	✗
Throughput	✓	✗	✗	✗	✓	✓	✗	✓
Transparency	✓	✓	✓	✓	✓	✓	✓	✗
Deployment	✓	✓	✓	✓	✓	✓	✗	✓

Table 1: Comparison of IODA to state-of-the-art approaches. IODA *achieves performance determinism without sacrificing throughput, and is transparent to applications with minimal device-side changes for easy deployment.*

tations, but introduce another question of *when* every device must start/stop GCs.

In terms of *which layer* tames the SSD performance issues, vast research has been done, from device-only modifications [9, 25, 42, 50–52], host-level changes [31, 34, 35, 53, 54], transparent approaches on programmable devices [11, 24, 38, 55, 56], to interface solutions [17, 49, 57–59]. Device-level proposals usually require vendors to significantly modify the firmware policies, thus not attractive for quick deployment; host-only optimizations can only guarantee a soft contract (*i.e.*, not eliminating background interferences); transparent approaches do not work for commodity SSDs, and many interface-level solutions focus on various types of inefficiencies of the existing software/hardware stack. Fortunately, IOD-PLM interface has been accepted and time is ripe for us to build solutions on it. IODA builds on top of the standard NVMe IOD-PLM interface and only requires minimal firmware changes for easy deployment.

The emerging Zoned Namespace (ZNS) [58] interface offers new opportunities for predictable performance by delegating more device controls to the host, but it could still potentially benefit from IODA techniques to co-schedule housecleaning tasks (*e.g.*, GCs) and the hardware across devices. We leave more detailed study as future work.

TTFLASH [9] tackles a similar problem as IODA. However, IODA's design context, principles, and technical challenges are fundamentally different. TTFLASH is a device-level design while IODA focuses on host/device co-design with minimal interface changes (we must address host-level and minor device-level changes and the interface design). TTFLASH requires extensive controller/firmware re-architecting, which we argue is not realistic (*e.g.*, reliance on NAND "copybacks" to enable chip-level blocking GC but skipping ECC checking) IODA does not enforce a specific GC policy. More importantly, IODA tackles a new problem of PLM management on IOD devices, we must address PLM limitations, design and build the needed software support in the host/OS.

Although several works on IOD begin to appear [13, 60], they mainly target hardware-level partitioning for better workload isolation, none of them address IOD-PLM challenges. We leave more detailed comparisons between IODA and related work in §5.2, qualitatively and quantitatively.

While these existing works without a doubt guide us to our ultimate solution, to the best of our knowledge, none of the works above answer the following questions: How can we extend and manage the existing IOD features and design proper software support to achieve always-predictable latencies? How should the host and the device agree on a proper PLM window to achieve an optimal result? How should the popular concepts of degraded reads and coordinated GCs be redesigned for future IOD-capable drives? Our unique contributions lie in answering the above questions.

3 IODA

We present IODA, an I/O deterministic flash array that is built on top of small and simple extensions around the existing IOD-PLM interface. This section describes our journey one step at a time towards reaching a highly deterministic latency and Section 3.4 puts all the pieces together.

3.1 Design Principles

When designing IODA, we adhere to the following goals and principles:

(a) *Make best-effort predictability stronger to guaranteed predictability.* The IOD-PLM concept is ideal for flash arrays if designed properly; the SSDs in the array can guarantee alternating internal activities and the host can leverage data redundancy for I/O reconstruction such that there is *no* single I/O that will be delayed by GC operations.

(b) *Continue reducing the host-SSD semantic gap.* For stronger predictability, we advocate SSDs to be "array-aware" with more but simple co-design/coordination between the OS and the devices without forcing the device to expose much of its internal proprietary information.

(c) *Make predictability more fine-grained.* To achieve a more efficient array, coarse-grained predictability mode (at the whole device level) should be augmented with finer-grained predictability at the I/O level to alleviate unnecessary reconstruction/rerouting overhead.

(d) *Limit device-level modifications and keep most of the complexity in the host.* Deployed flash firmware has gone through years of development, hence should not be heavily re-architected. All needed is for the firmware to shift its internal activities over time (*e.g.*, <100 lines of change). Similarly, applications should not be modified, leaving the OS to handle all the complexity of guaranteeing strong predictability.

3.2 PL_{IO}: Predictable-Latency Flagged I/Os

Our first method is to introduce **PL_{IO}**, *predictable-latency flagged I/Os*, by piggybacking a *binary* PLM query within the I/O submission command ("Will this I/O be predictable? Yes/No"). This allows a more live response of the predictability status. In other words, to have deterministic latency, the host ideally should know which I/Os that will be delayed

internally by the device such that the host will perform a degraded read without waiting. PL_{IO} binary response serves as a timely and accurate signal for the host to initiate proactive reconstruction. PL_{IO} modifications to the (a) interface, (b) firmware, and (c) host is minimal:

(a) At the NVMe interface level, we extend the I/O submission command with a 2-bit PL **flag** (using a slot in the existing 64 reserved bits). The purpose of this bit is as follows. For every user I/O, the host can mark them with PL=true (01) hinting to the underlying device that "ideally" this I/O should exhibit a predictable latency (not queued behind GC activities). If predictability cannot be guaranteed, please acknowledge the host as soon as possible. In our flash array setup, we initially set all read I/Os with PL=true.

(b) On the device side, when a user I/O contends with GC, the device firmware should *quickly* "fail" this unpredictable I/O by placing PL=fail (11) in the corresponding completion command. Afterward, the host can proactively reconstruct this unavailable block from the other devices in the array (§2). Otherwise, if GC is not active, the device can serve and complete the I/O without changing the flag (*i.e.*, the same processing logic as normal I/Os).

(c) On the host side, upon receiving a failed I/O, if the I/O is a read operation, the host can simply reconstruct the unavailable block by submitting additional I/Os with predictability off (PL=false (00)), which we call *reconstruction I/Os* to differentiate from the original user I/Os. After reconstruction, the host can return the user I/Os to the upper layers (*e.g.*, file systems) and deem it completed.

3.2.1 Benefits and Limitations. This simple extension delivers a large benefit for two reasons. First, failing an I/O only takes $1\mu s$ through PCIe and the xor-based reconstruction takes less than $10\mu s$ on modern CPUs. Thus, this fast response (plus reconstruction) can provide a significantly faster response than waiting for background operations to complete. The PL flag serves as a proactive signal to coordinate the device and the host on the correct timing to respond to the non-determinism. Second, the probability that more than one **sub-IOs** of the same stripe are delayed by simultaneous GCs on different devices is significantly lower than the probability of just one sub-IO getting delayed. A sub-IO is a page I/O within a full-stripe I/O. In a 4-drive array, a full-stripe I/O has 4 sub-IOs, including the parity page. We observed this probability in a detailed profiling experiment in the Linux block layer with real SSDs.

A limitation of this approach is that it can only reconstruct k sub-IOs within a stripe where k is the number of parity blocks (*e.g.*, k=1 in RAID-5 and k=2 in RAID-6). Thus, it is still tail-prone when $>k$ sub-IOs are not predictable (*i.e.*, the reconstruction I/Os also cannot be served quickly). The subsequent sections will address this limitation and show how PL_{IO} can be more powerful under further enhancement.
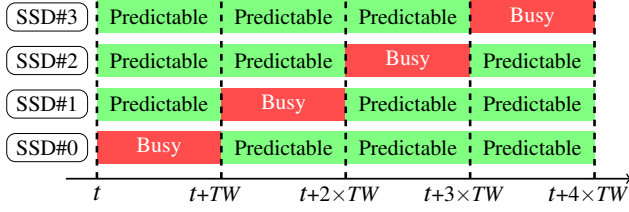
Figure 1: Alternating busy/predictable windows (§3.3).
This figure, using a 4-drive RAID-5, shows that in any time window (a duration of TW), there is at most one device in the busy mode, performing GC activities.

3.2.2 A Further Extension (PL_{BRT}).
To address the limitation of PL_{IO}, we explored extending the firmware furthermore to return the **"busy remaining time"** (**BRT**) to inform the host how long the corresponding I/O would have to wait. Thus, when multiple, n sub-IOs are returned with unpredictable flags (PL=11), including the reconstruction I/Os, the host will resubmit $n-1$ of the sub-I/Os with the *shortest busy remaining time*. This time, these I/Os must be resubmitted with PL=00 to avoid recursive fast-failures (*i.e.*, these I/Os will wait for GCs if any). In the firmware, calculating the BRT that affects a particular incoming I/O can be done in a straightforward fashion because it is about the chip and channel-level queueing delays with established device-level specifications. In the NVMe interface, we piggyback the busy remaining time in the NVMe completion command of the affected I/Os (using the 64 reserved bits).

Later in the evaluation, we show that PL_{BRT} improves upon PL_{IO}, but PL_{BRT} fails to provide a strong predictability contract. The PL_{BRT} technique works effectively under a low probability of multiple I/Os in a stripe delayed by concurrent background operations. However, we observed that in some deployments of a major storage company, the flash array design absorbs user writes to a separate battery-backed DRAM and flushes them in large sequential full-stripe writes across the SSDs. Hence, all the SSDs in the array *age at the same pace*, and because the device models are usually the same (*e.g.*, same firmware logic), GC operations kick in at relatively the same time. PL_{BRT} becomes ineffective here because the host would see multiple unpredictable I/Os with *similar* busy remaining time values.

3.3 PL_{Win}: Busy Latency Windows

3.3.1 Overview.
To provide a strong predictability contract, we leverage the fact that the notion of "PLM windows" has been accepted in the NVMe specification, *i.e.*, a device should alternate between busy and predictable windows. We take this concept within the context of flash arrays. Here, we concisely introduce the *rules to achieve strong predictability:*

(1) During the **busy time window** (*TW*), the device must have time to reclaim enough space via GCs and bring back the free over-provisioning space to a certain level (some percentage of the total raw NAND capacity) to serve the incoming writes during the predictable window.

(2) During the **predictable time window**, which lasts ($N_{ssd} - k$) × *TW* (explained later), every device must have enough over-provisioning space to absorb the largest possible write bursts to the device, hence guaranteeing no GCs are triggered during the predictable window.

Figure 1 illustrates the goal of using *TW* in a 4-drive RAID-5 array. In the first time window, between time t to $t+TW$, device #0 enters the busy mode for *TW* and performs GC to create a large free space in the over-provisioning area, which is crucial for absorbing the maximum write bursts during the predictable window. It's important to note here that the other devices (#1-#3) must be in the predictable mode and may *not* perform any GC. In the next time window, between $t+TW$ and $t+(2×TW)$, device #0 switches to predictable mode while device #1 enters its busy period (taking its turn to do GC operations). In this 4-drive RAID-5, every device must be able to sustain user write bursts within the predictable duration ($3×TW$) without triggering internal busyness. Note that writes are allowed during both the predictable and busy windows as we do not perform any write throttling or orchestration/staging which limits write throughput. To generalize the *TW* synchronization across SSDs, given an array's width (N), start-time (t), and *TW*, the ith SSD will enter its busy state at time ($t + (i - 1 + k × N) × TW$) for k in [0, 1, 2, ...]. Each SSD can use the controller's timer to perform busy/predictable state transitions *periodically* (e.g., via timer events) and autonomously without overlapping with other SSDs.

While similar coordination ideas as in Figure 1 have appeared in scenarios ranging from in-device RAIN [9, 19, 61] to even distributed "Java GC" [62, 63], we are not aware of existing works that apply it to flash array designs. The unique challenge here lies in programming the proper PLM windows without breaking the predictability contract. In this context, we need a configurable framework to program and formulate the busy window that IOD arrays can base on. For example, an SSD vendor employing a certain GC policy can slightly tune the formula/parameters to achieve the ideal window length for their SSD models; a flash array operator might want to relax the window value to better suit their target workloads for better device lifetime. To this end, we introduce **PL_{Win}**, *a TW formulation that flash array's host and devices can use to guarantee the contract*, hence making the flash array deliver predictable latencies all the time.

Due to the complex and proprietary GC dynamics whose details are invisible to the host for modern SSDs, devices are the ideal candidates to calculate the proper *TW* length and advertise them to the host. Host-based *TW* calculation would make more sense if devices are willing to expose more of the internals (*e.g.*, ZNS SSDs [58]).

3.3.2 TW Upper-Bound Formulation.
This section describes our *TW* formulation in a top-down fashion. To satisfy

$$TW \leq \frac{R_p \times S_t}{\left(N_{ssd} \times Min\left(B_{pcie}, Max\left(\frac{N_{dwpd} \times (1 - R_p) \times S_t}{8hours/day}\right)\right)\right) - \left(\frac{(1 - R_v) \times N_{ch} \times S_{pg} \times N_{pg}}{(t_r + t_w + 2 \times t_{cpt}) \times R_v \times N_{pg} + t_e}\right)}$$

Figure 2: The TW formulation. *The formula depends on 11 hardware-level parameters and 3 workload related parameters (the width of the flash array (N_{ssd}), R_v, N_{dwpd}). The breakdown of the formula is in Table 2.*

Symbol	Longer Symbol	Unit	Symbol Equation	Sim	OCSSD	FEMU	970	P4600	SN260
Hardware Time Specification									
t_{cpt}	TimeOfChannelPageTransfer	μs		40	60	60	40	60	60
t_w	TimeOfNandPageWrite	μs		2400	1440	140	960	2000	1940
t_r	TimeOfNandPageRead	μs		60	40	40	32	60	50
t_e	TimeOfNandBlockErase	ms		8	3	3	3	6	3
B_{pcie}	BandwidthOfPCIe	GB/s		4	8	4	4	8	8
Hardware Space Specification									
S_{pg}	SizeOfNandPage	KB		16	16	4	16	16	16
N_{pg}	NumberOfPagesPerBlock	.		512	512	256	384	256	256
N_{blk}	NumberOfBlocksPerChip	.		2048	2048	256	2731	5461	4096
N_{chip}	NumberOfChipsPerChannel	.		4	8	8	4	8	8
N_{ch}	NumberOfChannels	.		8	16	8	8	12	16
R_p	RatioOfOverProvisioning	.		0.25	0.12	0.25	0.20	0.40	0.20
R_v	RatioOfGCValidPages	.		0.5	0.75	0.7	0.75	0.75	0.75
Derived Values									
S_{blk}	SizeOfNandBlock	MB	$S_{pg} \times N_{pg}$	8	8	1	6	4	4
S_t	SizeOfTotalNandSpace	GB	$S_{blk} \times N_{blk} \times N_{chip} \times N_{ch}$	512	2048	16	512	2048	2048
S_p	SizeOfProvisionSpace	GB	$R_p \times S_t$	128	246	4	102	819	410
Garbage Collection									
T_{gc}	TimeToGCOneBlock	ms	$(t_r + t_w + 2 \times t_{cpt}) \times R_v \times N_{pg} + t_e$	658	617	57	312	425	408
S_r	SizeOfGCReclaimedSpace	MB	$(1 - R_v) \times S_{blk} \times N_{ch}$	32	32	2	12	12	16
B_{gc}	BandwidthOfGCCleaning	MB/s	S_r / T_{gc}	49	52	35	38	28	39
Workload Behavior									
N_{dwpd}	NumberOfCommonDWPD	.		10	10	40	10	10	10
B_{norm}	BandwidthOfWorkloadWrite	MB/s	$N_{dwpd} \times (S_t - S_p) / (8 \text{ hours})$	137	641	17	146	437	582
B_{burst}	BandwidthOfFullWrite	MB/s	$Min(B_{pcie}, Max(B_{norm}))$	3200	4000	536	3200	3204	4000
RAID									
N_{ssd}	NumberOfSSDsInTheArray	.		8	4	4	8	4	4
Time Window									
TW_{norm}	TimeWindowNormal	ms	$S_p / (N_{ssd} \times B_{norm} - B_{gc})$	6259	5014	6206	4622	24380	9171
TW_{burst}	TimeWindowBurst	ms	$S_p / (N_{ssd} \times B_{burst} - B_{gc})$	256	790	97	204	3279	1315

Table 2: Time window (TW) breakdown and values (§3.3). *The top row segments are basic NAND/controller-level parameters (i.e., "Hardware Time/Space Specification"), and the bottom row segments (i.e., "Derived Values, Garbage Collection, down to Time Window") are calculated based on the upper rows. We show analysis results for 6 SSD models (the right-most columns).*

the contract rules, TW must satisfy the following constraint:

$$TW \leq S_p / ((N_{ssd} \times B_{burst}) - B_{gc})$$

Without losing generality, let's consider a "*full cycle*" of $N_{ssd} \times TW$ as illustrated from time t to $t+(4 \times TW)$ in Figure 1 for one SSD in the array. B_{burst} represents the "*per-device maximum user write burst*", which we will break down in the subsequent section. The SSD is only allowed to perform GC on its own turn (in one TW), while writes can keep coming within the full cycle without any throttling/arbitration until the SSD has a chance again to perform GC. Thus, $N_{ssd} \times B_{burst}$ represents the maximum user write burst within a cycle for one SSD. Within its time window, the SSD can run GCs freely to reclaim space, say at the speed of B_{gc} (expanded later). This means $(N_{ssd} \times B_{burst}) - B_{gc}$ is the *net write load* that an SSD should handle in a cycle. In other words, the net incoming write load should not take up all the free over-provisioning space (S_p) that the SSD has.

All combined, the time window length (TW) must be less than the size of the over-provisioning space (S_p) divided by the net write load, hence the constraint above. Given that S_p is typically a fixed size, TW is mainly decided by N_{ssd}, B_{burst} and B_{gc}. For example, under a wide array (large N_{ssd}), TW must be set smaller to avoid breaking the IOD contract (will be analyzed further later).

TW has a lower bound, the latency of the smallest, non-preemptible unit of GC activity (T_{gc}). For example, a firmware might prefer to clean one NAND block as an uninterruptible activity to reclaim enough space within one TW.

3.3.3 TW **Parameters.** We now break down our *TW* formulation in a bottom-up fashion. The parameters we introduced (S_p, B_{burst} and B_{gc}) are high-level parameters that must be derived from hardware specifications. Figure 2 shows our final *TW* formulation that requires 11 hardware-level parameters. For understandability, we break down this equation in Table 2. The first row segment of Table 2 lists the hardware *time*-related specification such as channel transfer (t_{cpt}), NAND write (t_w), read (t_r), and erase (t_e) time and the host-device PCIe bandwidth (B_{pcie}). The second segment lists the hardware *space*-related specification such as the page size (S_{pg}), pages per block (N_{pg}), blocks per chip (N_{blk}), chips per channel (N_{chip}), number of channels (N_{ch}), over-provisioning ratio (R_p), and the average ratio of valid pages in victim blocks (R_v). These low-level parameters are needed to derive higher-level parameters (the third row segment) such as block size (S_{blk}), total NAND size (S_t), and over-provisioning space (S_p). From here, we can calculate GC behavior (the fourth row segment) such as the time to clean one victim block (T_{gc}), the size of the reclaimed space (S_r), and GC cleaning bandwidth (B_{gc}). The device also needs to understand the workload intensity, such as the maximum write bandwidth (B_{burst}) which depends on two values (B_{pcie} and B_{norm}). More importantly, *TW* depends on the width of the flash array (N_{ssd}).

3.3.4 TW Example Values. With all these parameters, we can set *TW*=TW_{burst} (the last row in Table 2) to fully guarantee the contract. To get a sense of the actual possible values, columns 5–10 of Table 2 show parameters of 6 SSD models we analyzed, including a simulated device that mimics a consumer SSD ("Sim"), a flash emulator used for our firmware prototyping ("FEMU") [23], an OpenChannel-SSD ("OCSSD") [24] whose parameters are publicly known, and 3 commercial SSDs from different vendors. We used an SSD prober to profile the hardware parameters of the commercial SSDs. Some of the SSD internal parameters are known to be "guessable" based on the observed latencies [64]. The average number of valid pages in a victim block (R_v) is estimated from running our workloads (§5) in FEMU [23] and OpenChannel-SSD [24]. We emphasize that the use of these numbers are only for analyzing possible *TW* values on real devices. Optionally, a more detailed version of Table 2 can be found in the Appendix (Table 2), covering all the drived
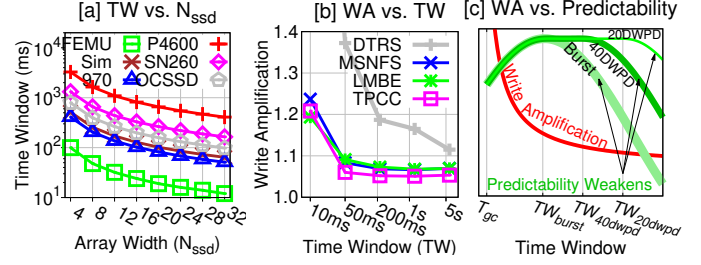

Figure 3: Time window analysis. *Figure (a) shows that TW can scale well to large arrays (e.g., >20 devices); Figure (b) demonstrates improved WA under larger TW; and Figure (c) presents the tradeoffs to balance WA, predictability and TW.*

values for the *TW* parameters.

Overall, when varying the number of devices (N_{ssd}) in the array from 4 to 8, TW_{burst} can range from ~100ms to ~3secs for different SSD models, which gives us a reasonable window length large enough to run sufficient GCs. Higher capacity devices such as enterprise SSDs can have a longer predictable window length, primarily because they have more over-provisioning space to absorb the incoming write burst, but the maximum user write burst (B_{burst}) is also limited by the PCIe bandwidth.

3.3.5 TW Scalability & Write Amplification (WA). We now analyze the trade-offs of *TW* values. Figure 3a shows the implication of larger array width (x-axis) to the *TW* value (y-axis) of 6 device models in Table 2. A *wider* array (larger N_{ssd}) forces *TW* to be *lowered* as the predictable window duration ($N_{ssd}\times TW$) for every device increases while the busy window period remains the same ($1\times TW$). This means the over-provisioning space will be full relatively faster.

Unfortunately, as shown in Figure 3b, a *lower TW* (in x-axis) causes a *higher* write amplification (**WA**) factor (in y-axis). Here we ran various workloads on SSD model "Sim" (more in §5.3.7). Let's take an example of *TW*=100ms in a 4-drive RAID-5 array, which implies a 300ms of predictable window length for each device. However, user write workload is typically *less intensive* than the maximum possible write burst, thus the over-provisioning space might *not* be full after 300ms, but yet the device is *forced* to transition to the busy window and start cleaning despite not many pages to clean, which then increases WA.

3.3.6 A More Relaxed Contract to Reduce WA. With the above analysis, a flash vendor/operator might worry about the unnecessary high WA given a small *TW* value. A preferable way is to absorb as many (over)writes until the over-provisioning space is almost full before starting GC. To incorporate this, the flash array can reuse our formulation but replace the maximum write burst (B_{burst}) with a typical "normal" user write throughput (B_{norm}). An industry standard to set this number is by using the drive-write-per-day metric (DWPD) [65]. For calculating B_{norm} in Table 2, we use DWPD values of 10 to 40 (N_{dwpd}), often suggested to prolong

the device lifetime to 3-5 years [66].

Plugging in this value to the same formula will give us TW_{norm}. As shown in the two last rows of Table 2, TW_{norm} increases the busy window length by 6-64× (higher compared to TW_{burst}), hence a longer predictable window length. While this reduces write amplification, we must call this a "*relaxed*" (weaker) contract. The reason is that the user write intensity may jump higher than the expected B_{norm} bandwidth. This in turn will fill up the over-provisioning space quickly and force the device to trigger GC even when it's not supposed to (still in predictable mode). This will be a rare event if user workloads follow the suggested DWPD.

3.3.7 The WA and Predictability Tradeoff. As analyzed above, one might prefer to re-configure the TW to achieve low WA without breaking the predictability contract. Figure 3c illustrates the tradeoff between write amplification and predictability under different time window values (x-axis). While WA improves with larger TW (red line), the predictability guarantee weakens if the TW is excessively too large as GCs have to forcefully kick in. Thus, it's necessary to find the sweet TW spot/range that can satisfy both requirements.

Under a "Burst" workload (boldest green line), the predictability guarantee first increases (*i.e.*, delivering overall better tail latencies) starting with the lower-bound TW value of T_{gc}, and peaks around $TW=TW_{busrt}$, the tight upper-bound TW value under the maximum-possible burst load. As TW continues to increase, the predictability guarantee weakens/decreases. For a lighter load (*e.g.*, the 40 and 20 DWPD green lines), they show a similar predictability-vs-TW trend, but the peak predictability guarantee can sustain over a range of $TW \in [TW_{burst}, TW_{40dwpd}]$, or $[TW_{burst}, TW_{20dwpd}]$, respectively. Here, TW_{40dwpd} represents the calculated TW value based on Figure 2 with N_{dwpd}=40. Combining the red line WA trend, the flash array operators better switch the TW from TW_{burst} to TW_{40dwpd} for better WA if the workload intensity decreases from "Burst" to "40DWPD". To re-configure TW, all needed is an NVMe admin command to re-program the TW value for all the devices in the array), and it can happen at the granularity of time slices (*e.g.*, every few minutes) or per-workload, which flash array operators already have good control of. Furthermore, the OS can be strengthened to dynamically adjust TW based on load changes. However, when under bursts, unpredictability will still show up as the TW adjustment lags behind workload intensity changes.

3.4 Putting It All Together

In summary, we show that the two combinations of PL_{IO} + PL_{Win} creates a very efficient flash array that fulfills the two rules of the strong contract we mentioned in Section 3.3. When not combined, each of these two techniques has limitations (which we will evaluate later).

PL_{IO} only: As discussed before, this method advocates a "fail-if-slow" hardware design to enable host-level timely re-construction for better latencies. However, it does not prevent multiple sub-IOs within a stripe from concurrent GC delays in different SSDs, thus the inability to achieve predictable latency when multiple SSDs are busy.

PL_{Win} only: Although PL_{Win} by itself guarantees at most one busy SSD in every busy time window, this labeling is *too coarse-grained*, *i.e.*, an I/O destined to a busy SSD might not contend with the internal GC. Let us suppose a block read B_0 to a busy device D_0 that must read the data via channel #8 in D_0. Channel #8 may be idle because the GC activities currently are on the other channels. But because PL_{Win} *assumes the whole* device D_0 is busy (too coarse-grained), then the host will not send B_0 to D_0. As a result, B_0's data must be reconstructed by reading B_1, B_2 and the parity block P. In general, because the host will never send any I/O to an SSD in its busy window, the frequent parity-based reconstruction overhead (probabilistically 25% of the time in a 4-drive array) is unnecessarily too excessive.

IODA (PL_{IO} + PL_{Win}): When PL_{IO} and PL_{Win} are combined, the host will always send I/Os with PL=true (01) *even to* a device in the busy state. It is more opportunistic in a more fine-grained way—*predictability is per I/O, not the whole device (or partition)*. If the I/O going to the busy device is not contending with GCs, then no data reconstruction is necessary. Otherwise, the array will guarantee that every busy I/O (PL=fail (11)) can always be circumvented. With IODA design, we ensure that only non-deterministic I/Os contending with GCing channels in the busy SSDs will be fast-failed and reconstructed from other drives. The reconstruction I/Os are guaranteed to be predictable based on our PL_{Win} window formulation, so they will not bloat up the system with endless/nested extra traffic. Later in the evaluation, we show that IODA caps the extra load to only a small percentage (*e.g.*, 6% in Figure 9b, and with <10% fast-rejected reads in Figure 7 across all the workloads). The CPU overhead is negligible compared to GC-induced long I/O latencies. Given this per-I/O predictability, our final IODA design also does *not* degrade the original aggregate bandwidth (IODA bandwidth is close to the raw RAID-5 bandwidth).

Regarding, PL_{BRT} (the shortest-background-remaining-time strategy), as stated in Section 3.2, we no longer need it but will still evaluate it for SSD vendors who do not prefer SSDs to be array-aware. (In PL_{Win}, the TW calculation requires the SSDs knowing N_{ssd}, the number of devices).

Interface and control flow: To achieve PL_{IO}+PL_{Win}, we extend the NVMe IOD-PLM and submission/completion interfaces with only 5 simple fields. Upon array initialization, the host informs each of the devices three pieces of information, array type (*e.g.*, k=1 in RAID-5) and the array width via two new fields, (1) arrayType and (2) arrayWidth. Next, the device plugs in these values to program TW internally and returns the value via (3) busyTimeWindow field in the PLM-Query's response. (Device proprietary information is not

exposed to the host). During runtime, the host and the device can tag submission (and completion) commands with the (4) `PL` flag. For flexible array volumes, the host can submit a new `arrayWidth` and the devices can re-program the `busyTimeWindow`). Finally, the host and the devices communicate the (5) `cycle's start time` (t in Figure 1).

Write path: IODA does not change the way the host/array or device performs writes. Data are striped and each write will trigger the parity updates. For non-full-stripe writes, parity updates will trigger RAID-level read-modify-writes. In this case, the reads are tagged with the `PL` flag. Since writes usually tend not to be latency sensitive, IODA design mainly targets strong read performance predictability without degrading the array's aggregate write bandwidth. IODA does not rely on write staging/orchestration. The *TW* analysis in §3.3 holds true for the general case where writes can arrive at the devices in both predictable and busy windows freely. IODA also does not change the write semantic/crash-consistency of the array. For example, if Non-Volatile Memory (NVM) (*e.g.*, NVRAM [67] or Optane Memory [68]) is used, the host/array only needs to write data to the NVM and flush to the device later. Otherwise, writes are directly acknowledged either when hitting the in-device buffer or the NAND pages when device buffers are full. We acknowledge that NVM can be used as an effective caching layer and greatly improve average latencies; but the tail latencies which are often caused by cache misses, unfortunately, will not go away. For example, read misses will still contend with GCs (triggered by frequent flushes) at the SSD/array level. This is because write buffering (*e.g.*, using NVRAM) only removes user-level read vs. user-level write contention. With/without write buffering, user-level reads are still contending with GC-induced writes (which is our focus). Our current IODA prototype is built on top of the Linux "`md`" sub-system without NVRAM support.

Limitations and discussions: We assume the SSDs in the array are of the same model and size. The SSD vendors should be persuaded to implement our simple interface extension. While IODA currently concentrates on GC-induced non-determinism, it can be extended to handle other types of I/O contentions (*e.g.*, queueing delay, wear-leveling, flushing, etc.), apply to other types of array layout (*e.g.*, erasure-coded systems for more flexible busy window scheduling), and benefit new hardware determinism-capable designs via PL_{IO} (*e.g.*, head-of-line blocking in networking).

4 Implementation

We now describe IODA implementation [69].

IODA's firmware side: We prototype the firmware logic in two open-source SSD research platforms. **(a)** *FEMU (upgraded).* FEMU is a recent QEMU-based and DRAM-backed SSD emulator [23, 70] used by some recent works appearing in top venues [42, 43, 71, 72]. To make FEMU resemble modern SSDs, we had to make several optimizations in *1200*

LOC. Bottom line, our FEMU version can deliver 400 KIOPS throughput and as low as 10µs I/O latency. On top of this, we then built a firmware that returns the `PL` flag and performs GC only in the busy window, all only in *60 LOC*. **(b)** *LightNVM+OCSSD.* We also prototype IODA with LightNVM on a real OCSSD [24, 73] in 186 LOC for additional evaluation. One design flaw of our OCSSD controller is that it excessively favors reads over writes (*e.g.*, write throughput drops to only 3MB/s under a 2:1 read/write mixed workload). To address this issue, we re-architected LightNVM with a per-chip FIFO queue in 780 LOC.

IODA's host side: The host-side logic is written in *1814 LOC* in Linux 4.15 Software RAID (*i.e.*, the Linux `md` subsystem) and *18 LOC* in the NVMe driver. While the LOC is small, it took us a long time to address many hurdles in the complex Linux storage stack such as the intricate timeout/retry mechanism, the `NVMe/BIO/request` I/O `PL`-flag passing, and the complex Linux RAID per-stripe state machine.

Re-implementation of other works: It is important to compare IODA comprehensively, but because other works use varying platforms (some even cannot run), "apples-to-apples" comparison would be difficult to make. With our upgraded FEMU, we were able to re-implement state-of-the-art techniques [25, 29, 31, 33, 35] in around *3400 LOC*.

5 Evaluation

We present our comprehensive evaluation in three sections: We first show the main results of latency determinism brought by IODA approaches under various workloads (§5.1). Then we present comparisons of IODA with the state of the art (§5.2) and show extended evaluations (§5.3).

Platform setup: Most experiments are done on FEMU (for reasons mentioned in §4) running on Emulab D430 machines [74]. We run Linux Software RAID-5 (4KB chunk size) on 4 FEMU drives. The LightNVM+OCSSD full-stack setup is similar and done on our local lab machine.

The FEMU's base firmware uses a page-level dynamic mapping and a greedy-GC policy for best cleaning efficiency. GCs are triggered upon reaching a pre-configured high watermark (25% of free blocks available). GCs will forcefully run at full speed under the low watermark (5%) to ensure enough free space for user requests. The device parameters were detailed in the "FEMU" column in Table 2. We configured FEMU to emulate modern low-latency SSDs (*e.g.*, Z-NAND [75]) with SLC-like access latencies (*i.e.*, ~200µs for writes), faster than existing MLC/TLC SSDs analyzed in Table 2. Later, we show that IODA evaluations on our MLC-based OCSSD show the same conclusion as FEMU.

Macrobenchmarks: For block I/O traces, we use 4 SSD traces from Microsoft data centers, spanning cloud storage (`AZURE` and `COSMOS`), search engine (`BingIdx`) and database workloads (`BingSel`) and 5 standard SNIA block traces [76] that we have re-rated 8-32 times more intense to reflect mod-
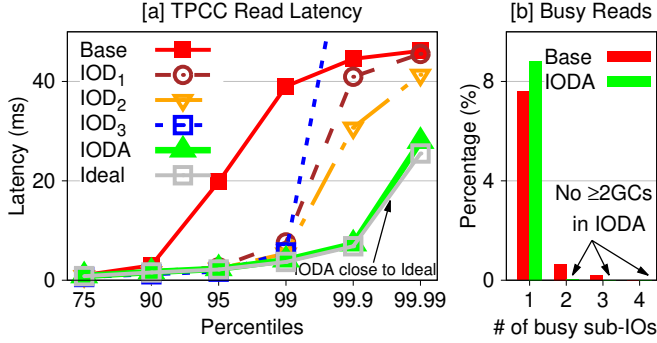
Figure 4: IODA percentile latencies and #busy sub-IOs with TPCC (§5.1.1). *Figure (a): read latencies (y-axis) at major percentiles p75 to p99.99 (x-axis) with various IODA strategies. Figure (b): the percentage of stripe-level reads (y-axis) that experience 1 to 4 busy sub-IOs (x-axis).*

ern SSD workloads, all characterized in Table 3. In these traces, we pick the 1-hour busiest period. For real applications, we run 6 Filebench workloads [77] and 3 YCSB/RocksDB workloads [78] on the ext4 file system. Additionally, we also run 12 other storage workloads ranging from GNU applications, Sysbench [79], to MapReduce (Hadoop/Spark) workloads [80]. All user I/Os are marked as latency sensitive (PL=true (01)).

Metrics: We primarily report read latencies for the block traces and application-specific metrics for the rest (*e.g.*, average latencies, runtime, etc.). We also analyze other aspects of IODA design (*e.g.*, write latency and throughput). Each experiment is repeated and ran for a long period with thousands of GCs triggered over FEMU drives in steady state, showing consistent results. Finally, **pYY** implies the *YY^{th} percentile*.

5.1 Main Results

This section shows the improvement made by the combination of IODA strategies, one at a time: "IOD$_1$" represents only predictable-latency flagged I/Os (PL$_{IO}$ in §3.2), "IOD$_2$" the shortest-busy-remaining-time strategy (PL$_{BRT}$ in §3.2), "IOD$_3$" the alternating busy windows *only* (PL$_{Win}$ in §3.3, *without* PL$_{IO}$/PL$_{BRT}$), and "IODA" the final approach (PL$_{IO}$+PL$_{Win}$ as described in §3.4). For IOD$_3$ and IODA, our FEMU-based firmware uses a busy time window of 100ms as calculated in Table 2. We also show "**Ideal**" to represent an ideal performance where there are no GC-induced latencies, by disabling GC delay emulation in FEMU.

5.1.1 IODA Techniques, 1 Workload First. For figure simplicity, we first show only the results of using one workload, TPCC (Table 3). Figure 4a shows the latencies at major percentile values (p75 to p99.99) of five different approaches: **(0)** The red Base line represents the TPCC workload without any strategies. Starting at p95 (x=95) the Base's latency is no longer deterministic, consistent with what we observe on real commodity SSDs. **(1)** The brown IOD$_1$ line shows that by
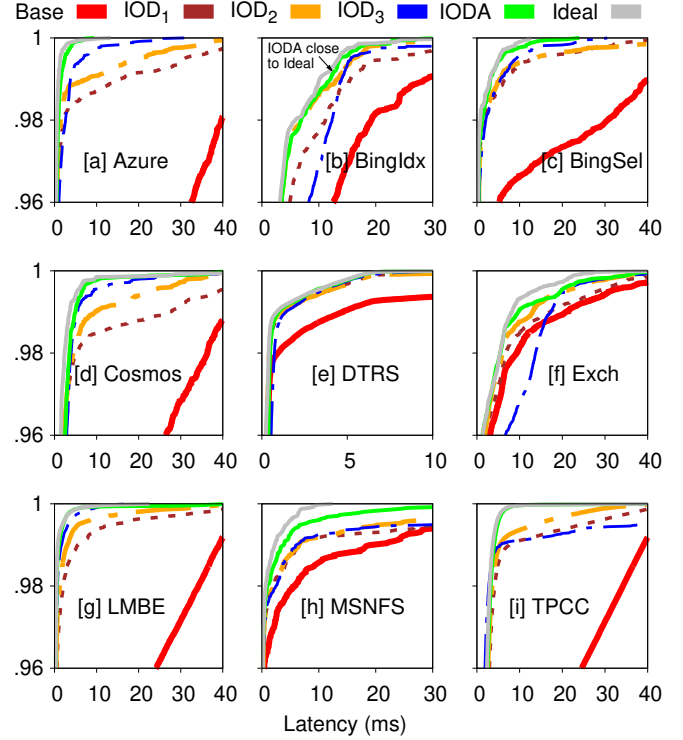

Figure 5: Read latency CDFs for all 9 block I/O traces (§5.1.2). IODA *is the closest to the ideal case across all 9 block trace workloads.* IOD$_2$ *improves over* IOD$_1$*, but could not eliminate concurrent GC blockings.* IOD$_3$ *is worse than* IODA *due to whole-device level busy state.*
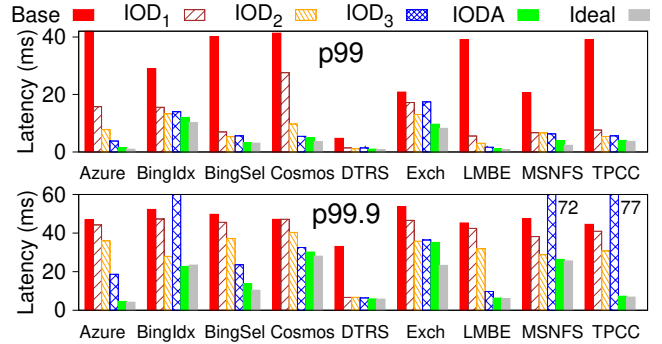

Figure 6: p99 and p99.9 latencies (§5.1.2). *This figure details the p99 and p99.9 latencies from different I/O traces under all* IODA *strategies.* IODA *is the most deterministic and almost reaches the* Ideal *values.*

just circumventing the busiest (slowest) read, via proactive data reconstruction as signaled by the PL$_{IO}$ method, the latency is more predictable up to p99. **(2)** The orange IOD$_2$ line shows that the PL$_{BRT}$ busy-remaining-time approach further helps but cannot completely evade concurrent busyness. **(3)** The blue IOD$_3$ line shows that PL$_{Win}$-only method is stable up to p99 but it is expensive (spikes at p99.9 and higher) due to the excessive and unnecessary data reconstruction
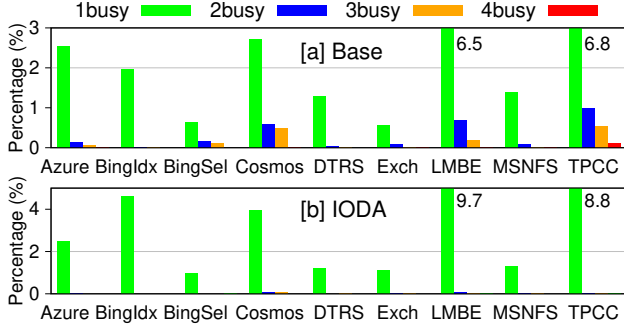
Figure 7: #Busy sub-IOs, many I/O traces (§5.1.2). *The figure is the same type as Figure 4b, but now with many I/O traces. IODA shifts multiple concurrent* `2-4busy` *sub-IOs (in the top* `Base` *figure) to more* `1busy` *sub-IOs (in the bottom* `IODA` *figure).*

Trace Workload	#I/Os (K)	Read/Write (%)	Read/Write (KB)	Max I/O (KB)	Interval (µs)	Size (GB)
`Azure`	320	18/82	24/20	64	142	5
`BingIdx`	169	36/64	60/104	288	697	11
`BingSel`	322	4/96	260/78	11264	2195	24
`Cosmos`	792	8/92	214/91	16384	894	63
`DTRS`	147	72/28	42/53	64	203	2
`Exch`	269	24/76	15/43	1024	845	9
`LMBE`	3585	89/11	12/191	192	539	74
`MSNFS`	487	74/26	8/128	128	370	16
`TPCC`	513	64/36	8/137	4096	72	25

Table 3: Block I/O trace characteristics (§5.1). *This table shows the detailed characteristics of the block traces we use.*

(§3.4). **(4) [Key result #1]** *Finally, the bold green* `IODA` *line in Figure 4a shows that* $PL_{IO}+PL_{Win}$ *provides the best latencies. The thin gap between the* `Ideal` *and* `IODA` *lines shows the power of* IODA *in being latency deterministic. Even at* ***p99.99**, IODA is only **9%** slower than the ideal performance.*

Figure 4b reveals the reason behind IODA's success. The x-axis shows how many "sub-IOs" of a stripe are returned busy (`PL=11`, §3.2). At x=1, the `Base` bar shows that roughly 7% of stripe-level I/Os experience 1 busy sub-IO, but the base approach just waits for (does not reconstruct) busy sub-IOs. At x=2, `Base` shows that almost 1% of the stripe-level reads experience 2 busy sub-IOs. While IOD_1 and IOD_2 can reconstruct 1 busy sub-IO, it cannot evade this concurrent busyness. That is why the IOD_1 and IOD_2 lines in Figure 4a start increasing between the p99 and p99.9 values. **[Key result #2]** *With our final approach, the green* `IODA` *bar in Figure 4b shows that our time-window approach successfully* ***shifts*** *concurrent GCs across time such that at any time there is at most only one busy sub-IO per stripe.* Hence, the `IODA` bar is higher than the `Base` bar, reaching y=8% at x=1 but y=0 at x>1 (acceptable given the reconstructability).

5.1.2 Many Workloads (Block I/O Traces). Figure 6 shows the p99 and p99.9 latencies with all the block traces. Figure 5 displays the complete read latency CDF graphs. [Key result #3] *Overall, with all these experiments with different workload characteristics and base latency distributions, the* `IODA` *bars in Figure 6 and CDF lines in Figure 5 summarize that* IODA *delivers faster latencies, 1.7× on average up to 16.3× between p95–p99.9 compared to the base approach, and only 1.0× to 3.3× slower than the* `Ideal` *case.*

Figure 7 shows the percentage of stripe-level reads that observe busy sub-IOs (from `1busy` to `4busy`), the top and bottom figures represent the percentage for the baseline and IODA, respectively. Similar to Figure 4b, it shows that IODA successfully shifts the concurrent GCs across time (higher `1busy` green bars with almost no `2-4busy` bars).

5.1.3 File System, Key-Value, and Other Applications. We also ran various applications on ext4 on IODA, including

6 Filebench workloads, 3 YCSB/RocksDB workloads, and a dozen of data-intensive and stand-alone applications. The results are summarized in Figure 8, *all pointing to the same key conclusion that* IODA *is near to the ideal scenario.*

5.2 Versus State-of-the-Art Approaches

For readability, this section mainly compares IODA with state-of-the-art approaches using one benchmark TPCC; other workloads show the same conclusion. All the results are aggregated in Figure 9.

5.2.1 vs. Proactive/Cloning (Always Full Stripe I/Os). A simple black-box way to cut 1-busy sub-IOs is to always proactively send a full-stripe read including the parity read (akin to cloning [2, 45, 81]), hence the I/Os can return to the user when the first ($N_{ssd}-k$) sub-IOs finish. Figure 9a shows that `Proactive` is effective *but* still loses to IODA at high percentiles due to its inability to evade concurrent busy sub-IOs. `Proactive` also *negatively adds more load*. Figure 9b shows `Proactive` inefficiently sends down 2.4× more I/Os to the base case, while `IODA` only issues 6% more reads.

5.2.2 vs. Synchronized GCs (e.g., Harmonia [33]). Synchronized GCs attempt to schedule the SSDs in an array to reduce GC impacts [33, 34, 49]. For example, Harmonia [33] manages the SSDs to perform GCs at the *same* time (*i.e.,* a localized slowdown is better than scattered ones). Figure 9c shows that Harmonia [33] improves the overall average latency by 27% compared to the baseline, *but* is far from achieving latency determinism due to the localized slowdown. IODA's alternating window strategy is more superior.

5.2.3 vs. Partitioning (e.g., Flash on Rails [35]). Flash on Rails (Rails) [35] partitions the SSDs such that user-vs-GC or user-vs-user contention is reduced. It divides an array into read-only and write-only SSDs, and performs read-write role swapping periodically. A similar strategy can also be found in Gecko [48] and SWAN [34]. Figure 9d shows that Rails is indeed able to deliver a pure read-only latency (the left-most orange line). The "raw" IODA (the right-most line) loses because *Rails relies on much NVRAM* to stage all inflight writes.
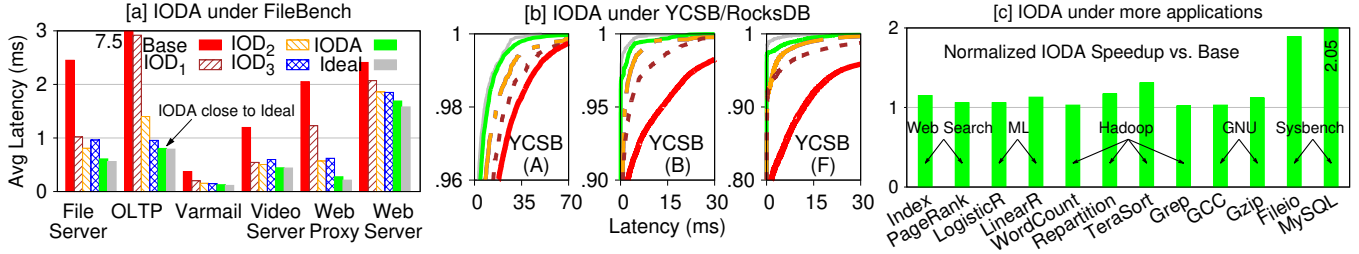
Figure 8: Filebench, YCSB, and other standalone/misc data-intensive application results (§5.1.3). *Figure* **(a)** *shows the average latencies of six Filebench workloads as Filebench doesn't support per-IO latency logging.* IODA *is the most optimum and nearest to* Ideal*; Figure* **(b)** *presents latency CDFs for three YCSB workloads (A, B, and F), and again,* IODA *almost reaches the* Ideal *performance at high percentiles; Figure* **(c)** *shows the end-to-end normalized performance improvement (*IODA *vs.* Base*) based on workload-specific performance metrics (e.g., runtime, latency/throughout, etc.)*
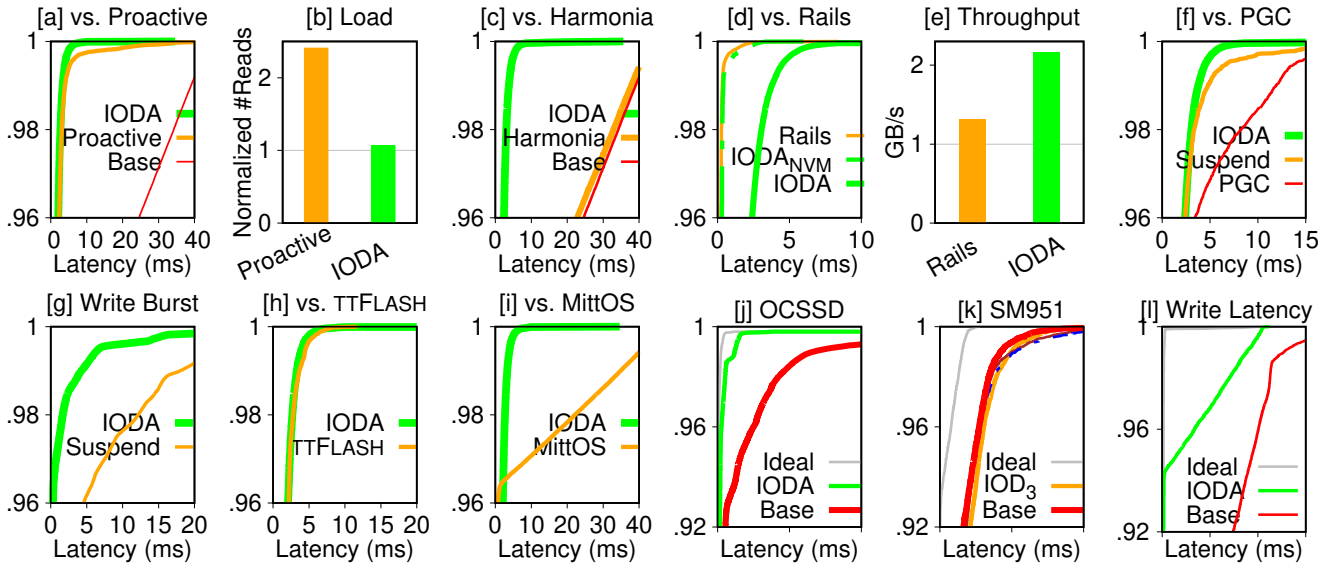

Figure 9: IODA vs. 7 state-of-the-art approaches (§5.2) and extended evaluations (§5.3). *In Figure* **(a)**–**(i)**, IODA *outperforms almost all the 7 competing approaches in delivering predictable I/Os without sacrificing array bandwidth, burdening the system with excessively extra load, or requiring excessive host-side buffering or device-side changes. Figure* **(j)**–**(l)** *show* IODA *extended evaluations on OpenChannel-SSD (OCSSD) and commercial (SM951) SSDs, and write latency:* **(j)** IODA *achieves predictable latencies on a real OCSSD (§5.3.1),* **(k)** *how unmodified commodity SSDs requires our proposed device-level modifications (§5.3.3).* **(l)** IODA *improves write latencies by virtue of improved read latencies for the read-modify-write parity update process (§5.3.5).*

In "raw" IODA, however, user reads are queued together with user writes. For a fair comparison, after we add a similar host-side write buffering, the $IODA_{NVM}$ line in Figure 9d shows roughly the same performance as Rails.

However, Rails has two *fundamental downsides: reduced throughput and requiring large NVRAM*. As SSDs are broken into read/write roles separately, there are *fewer* number of devices to serve reads (and writes). Figure 9e shows that Rails' throughput is significantly lower compared to IODA, underutilizing the array's bandwidth. Further, Rails requires much NVRAM to stage all incoming writes. The needed NVRAM is proportional to the write-mode duration and N_{ssd}, making it prohibitively too large for real systems.

5.2.4 vs. Preemptive GC. Preemptive GC (PGC) [25] is an approach that allows user reads to be interleaved in between

GC individual read/write/erase operations, hence user reads are not queued far behind. Compared to the Base latency, PGC has already successfully reduced a huge area of the latency tail. But, the IODA line in Figure 9f shows that, vs. PGC, IODA is still more effective. This is because IODA users do *not* need to wait for *any* individual GC operation, but PGC users *sometimes* must wait for *at least one* individual GC operation.

5.2.5 vs. P/E Suspension. To further improve preemptive GC, more recent works suggest program/erase (P/E) suspension, even in the middle of a GC write/erase operation [28, 29]. It will deliver more stable latencies by allowing reads to "interrupt" write/erase and resume it later (see Suspend vs. PGC in Figure 9f). IODA still outperforms the suspension method.

A fundamental weakness of GC preemption and suspension is that these features *must be disabled* when the over-
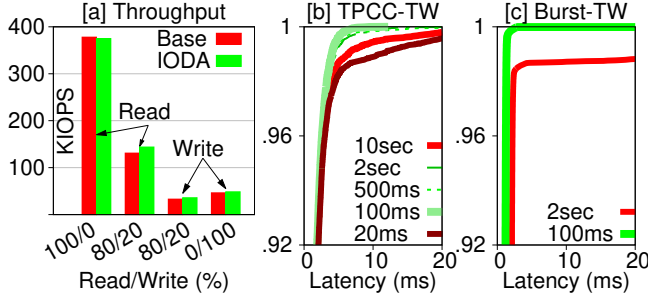
Figure 10: IODA throughput and performance sensitivities to *TW*. *(a)* IODA-*vs-Base read/write throughput under various read/write ratios (§5.3.5), **(b)** TW sensitivity on TPCC performance (§5.3.6), **(c)** same as (b) but under maximum write burst (§5.3.6).*

provisioning space is *full* (*e.g.*, under continuous write bursts). IODA's busy/predictable windows on the other hand alternate all the time. Figure 9g compares the performance of IODA and P/E suspension under a continuous maximum write burst. Here, we can clearly see that IODA's benefit is more apparent compared to the benefit of P/E suspension (the gap between the IODA and Suspend lines is larger in Figure 9g than in Figure 9f). **[Key result #4]** *Overall,* IODA *outperforms state-of-the-art methods in delivering deterministic latency, even under maximum write bursts.*

5.2.6 *vs.* TTFLASH.
TTFLASH [9] is a "tiny-tail" flash controller design by pushing GCs to a finer-granularity (*i.e.*, chip level) and perform them rotationally. We followed TTFLASH firmware organizations and implemented TTFLASH logics in FEMU. Figure 9h shows IODA can achieve similar predictable latencies as a RAID-5 array of four TTFLASH drives. However, TTFLASH's internal RAIN [61] layout shrinks per-drive capacity and throughput as one channel is dedicated for in-device parity maintenance (25% degradation, not shown). We would also like to further stress that IODA design achieves predictable I/Os without heavily re-architecting the flash firmware/controller as TTFLASH does (§2.3), thus distinguishing itself in its unique design context (host/device co-design), principles (simplicity for deployment), and technical challenges (PLM refinement and management, as well as host OS predictable I/O stack design).

5.2.7 *vs. MittOS.*
MittOS [38] advocates a SLO-aware interface to allow quick I/O fail-over to replicas for fast response. It relies on "open/white-box" device knowledge to make OS-level predictions, thus not applicable for commercial devices. As shown in Figure 9i, MittOS loses to IODA as I/O fail-over might also be slow if the target node/device is busy. IODA's PL$_{Win}$ approach eliminates the gap here. A side note, MittOS's I/O fast-rejecting interface is based on OS-level prediction to the underlying "profiled" devices, while IODA per-IO predictability flag (PL$_{IO}$) is lightweight and accurate with host/device collaboration.

5.3 Extended Evaluations

5.3.1 IODA *on OpenChannel-SSD (OCSSD).*
IODA approach also runs well on real SSD hardware. We re-implement IODA's firmware changes in the Linux Light-NVM driver ("host-side firmware") and run it on OCSSD [24]. Figure 9j shows a similar improvement as on FEMU, as shown earlier in Figure 4a.

5.3.2 IODA *on Light-NVM on "FEMU$_{OC}$".*
Unfortunately, our 5-year-old OCSSD became erratic and the vendor no longer supports/sells it; we could not complete more experiments on our OCSSD. This reality of real SSD hardware platforms is likely a reason why software-based flash emulators appear more recently in major venues [42, 43, 71, 72, 82]. Luckily, FEMU can also act as a drop-in replacement of OCSSDs for Light-NVM [23] (a host-managed "FEMU$_{OC}$" with the device firmware stripped). Table 4

	95th	99th	99.9th	99.99th
Azure	11.9	8.4	6.2	5.1
BingIdx	1.6	1.4	1.6	1.6
BingSel	3.7	3.1	2.3	1.9
Cosmos	9.2	5.6	1.8	1.4
DTRS		2.8	3.0	11.9	13.7
Exch	7.1	3.5	5.6	2.1
LMBE	16.0	8.0	1.9	1.3
MSNFS	1.4	2.8	12.1	6.3
TPCC	5.4	3.8	1.7	2.1
YCSB-A	7.3	3.1	3.5	4.7
YCSB-B	19.0	3.8	5.3	1.2
YCSB-F	6.8	4.4	7.2	5.4

Table 4: IODA Speedup vs. Base on top of FEMU$_{OC}$

shows the normalized latency improvement of IODA vs. Base at major percentiles across various workloads.

5.3.3 IODA *on Commodity SSDs?*
One might wonder whether IODA can be achieved on commodity SSDs without device-level modifications. We ran our *TW* algorithm, IOD$_3$ (PL$_{Win}$-*only* on the host side), on an array of real consumer SSDs. We set *TW* to 100ms, 1 and 10 seconds. Figure 9k shows that they are not effective and far from the Ideal line as commercial SSDs do not have the PL$_{IO}$ and PL$_{Win}$ mechanism in place to kindly signal the host for proactive reconstructions. **[Key result #5]** *This experiment strongly shows the necessity to add small firmware modifications to honor the predictable latency mode window.*

5.3.4 IODA *Write Latency.*
Back to the FEMU-based IODA, Figure 9l shows IODA benefits to write latencies. Each non-full-stripe write in RAID-5 triggers a read-modify-write process to update the parity page, hence user write latency is affected by the internal read performance. By virtue of predictable read latencies in IODA, write latencies are also significantly improved (up to p96 across all workloads, not shown). When user writes (or the associated parity updates) contend with device-level GCs, they might still get queued behind. That's the reason IODA write latency loses to "Ideal" for the last few percentiles.

5.3.5 IODA *Throughput.*
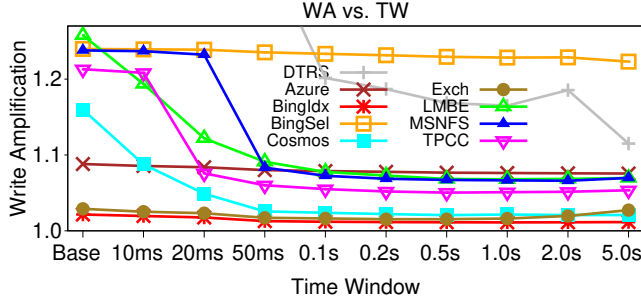Figure 10a shows the IODA and Base read/write IOPS under a 256-thread FIO benchmark

Figure 11: Write amplification sensitivity (§5.3.7). *The y-axis shows the write amplification factor (WAF) and the x-axis varies the TW value.*

Figure 12: Adjusting *TW* for predictability and low WA (§5.3.8). *This figures demonstrate how flash array operators can re-configure the TW to achieve low write amplification without sacrificing latency predictability.*

with various read/write ratios (100/0, 80/20 and 0/100). Note that the IOPS is capped by FEMU's throughput (§4). One interesting phenomenon here is that IODA improves the write throughput by 9% in the 80/20 and 0/100 R/W configurations similarly because IODA improves the read latency in read-modify-write parity operations. **[Key result #6]** IODA *does not sacrifice the raw RAID read/write throughput.*

5.3.6 Performance Sensitivity to TW Values. The current IODA setup uses *TW*=100ms based on the calculated value in Table 2 ("*TW_{Burst}*" row and "FEMU" column). Figure 10b shows the performance sensitivity under a smaller/larger *TW* value. The average load of the workload is ~13 DWPD (monitored at the device-level). If we calculate the *TW* value based on the *TW* formula in Figure 2, we get *TW_{norm}*=~5s, which is the upper-bound *TW* to guarantee the predictability contract. Under *TW*={500ms,2s} (*i.e.*, <5s), we can see that the green lines sticking together and all showing predictable latencies. However, if we further increase *TW*=10s, the SSDs *fail* to guarantee the absence of GC within the predictable windows, hence worse performance (*i.e.*, the SSDs couldn't reclaim enough space during the busy windows, and forceful/non-delayable GCs have to spawn into the predictable windows). This performance gap is more apparent in Figure 10c where we send a continuous *maximum* write burst that fills up the over-provisioned space faster. Under *TW*=20ms, we also see slightly worse performance (see "lower bound" in §3.3.2). As a result, some leftover disturbance is still felt after the device alternates to the predictable window.

5.3.7 Write Amplification Sensitivity to TW Values. To show the implication of various *TW* values to write amplification (WA), we ran a longitudinal analysis using an event-driven SSD simulator, SSDSim [83]. Figure 11 shows the result across different workloads and *TW* values. As expected, short windows (*e.g.*, 10ms) will cause high WA (*e.g.*, 1.2× or more) but long windows reduce the WA. Our 100ms busy window value for our emulated device delivers a reasonable WA (1.0 to 1.1× in most of the workloads). As discussed in §3.3.4, operators can use a practical DWPD value to increase window durations and reduce WA further.
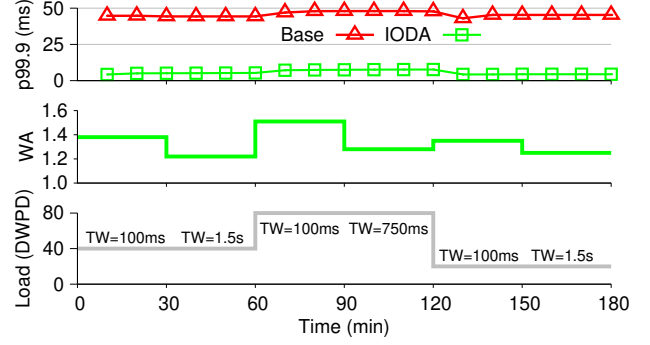
5.3.8 Re-configuring TW for better WA. As discussed in §3.3.7, flash array operators could dynamically adjust the *TW* for their target workloads to balance WA and predictability (*i.e.*, use *TW*=*TW_{norm}* instead of *TW_{burst}*). In Figure 12, we ran 3 synthetic FIO workloads with different write intensities (40, 80, and 20 DWPD) each for one hour. For each workload, we configure IODA to use *TW*=*TW_{burst}* for the first 30 minutes and *TW*=*TW_{norm}* for the second half. We report the p99.9 latencies (every 10 minutes) and write amplification factor (WA). From the top and middle figures in Figure 10, we can see that IODA can sustain predictable latencies while improving WA by switching to a larger *TW*.

6 Conclusion

IODA is a host/SSD co-designed flash array that provides a strong latency predictability contract without sacrificing the aggregate bandwidth. IODA only involves minimal changes to the NVMe interface and flash firmware to simplify deployment. IODA delivers close-to-ideal latencies and outperforms many state-of-the-art approaches. We hope IODA will spur more work around the new and exciting IOD-PLM interface.

7 Acknowledgments

References

[1] Luiz Barroso, Mike Marty, David Patterson, and Parthasarathy Ranganathan. Attack of the Killer Microseconds. *Communications of the ACM*, 60(4), 2017.

[2] Jeffrey Dean and Luiz Andre Barroso. The Tail at Scale. *Communications of the ACM (CACM)*, 56(2), 2013.

[3] Why Deterministic Storage Performance is Important. https://www.architecting.it/blog/deterministic-storage-performance/, 2018.

[4] All-Flash NVMe Reference Architecture. https://www.samsung.com/semiconductor/global.semi/file/resource/2020/05/redhat-ceph-whitepaper-0521.pdf, 2020.

[5] Micron 9100 U.2 and HHHL NVMe PCIe SSDs. https://www.micron.com/-/media/client/global/documents/products/data-sheet/ssd/9100_hhhl_u_2_pcie_ssd.pdf, 2020.

[6] Achieve Consistent Low Latency for Your Storage-Intensive Workloads. https://www.intel.com/content/www/us/en/architecture-and-technology/optane-technology/low-latency-for-storage-intensive-workloads-article-brief.html, 2021.

[7] Ross Stenfort, Ta-Yu Wu, and Lee Prewitt. NVMe Cloud SSD Specification. https://www.opencompute.org/documents/nvme-cloud-ssd-specification-v1-0-3-pdf, 2020.

[8] Storage Latency in Flash Arrays. https://www.violinsystems.com/wp-content/uploads/Storage-Mojo-WP-storage-latency.pdf, 2020.

[9] Shiqin Yan, Huaicheng Li, Mingzhe Hao, Michael Hao Tong, Swaminathan Sundararaman, Andrew A. Chien, and Haryadi S. Gunawi. Tiny-Tail Flash: Near-Perfect Elimination of Garbage Collection Tail Latencies in NAND SSDs. In *Proceedings of the 15th USENIX Symposium on File and Storage Technologies (FAST)*, 2017.

[10] Nima Elyasi, Changho Choi, Anand Sivasubramaniam, Jingpei Yang, and Vijay Balakrishnan. Trimming the Tail for Deterministic Read Performance in SSDs. In *IEEE International Symposium on Workload Characterization (IISWC)*, 2019.

[11] Jian Ouyang, Shiding Lin, Song Jiang, Zhenyu Hou, Yong Wang, and Yuanzheng Wang. SDF: Software-Defined Flash for Web-Scale Internet Storage System. In *Proceedings of the 19th ACM International Conference on Architectural Support for Programming Languages and Operating Systems (ASPLOS)*, 2014.

[12] GreyBeards on Storage. https://silvertonconsulting.com/gbos2/tag/tail-latency/, 2016.

[13] Chris Petersen, Wei Zhang, and Alexei Naberezhnov. Enabling NVMe I/O Determinism @Scale. https://www.flashmemorysummit.com/English/Collaterals/Proceedings/2018/20180807_INVT-102A-1_Petersen.pdf, 2018.

[14] Kapil Karkra. Using Software to Reduce High Tail Latencies on SSDs. https://www.flashmemorysummit.com/English/Collaterals/Proceedings/2018/20180808_SOFT-201-1_Karkar.pdf, 2018.

[15] Data Set Management Commands Proposal for ATA8-ACS2. http://www.t13.org/Documents/UploadedDocuments/docs2008/e07154r6-Data_Set_Management_Proposal_for_ATA-ACS2.pdf, 2020.

[16] NVM Express Base Specification 1.0. https://nvmexpress.org/wp-content/uploads/NVM-Express-1_0e.pdf, 2020.

[17] Taejin Kim, Duwon Hong, Sangwook Shane Hahn, Myoungjun Chun, Sungjin Lee, Jooyoung Hwang, Jongyoul Lee, and Jihong Kim. Fully Automatic Stream Management for Multi-Streamed SSDs Using Program Contexts. In *Proceedings of the 17th USENIX Symposium on File and Storage Technologies (FAST)*, 2019.

[18] NVM Express Base Specification 1.4. https://nvmexpress.org/wp-content/uploads/NVM-Express-1_4-2019.06.10-Ratified.pdf, 2020.

[19] Jon C. R. Bennett. Memory Management System and Method. https://www.google.com/patents/US8200887, 2012.

[20] K. V. Rashmi, Mosharaf Chowdhury, Jack Kosaian, Ion Stoica, and Kannan Ramchandran. EC-Cache: Load-Balanced, Low-Latency Cluster Caching with Online Erasure Coding. In *Proceedings of the 12th USENIX Symposium on Operating Systems Design and Implementation (OSDI)*, 2016.

[21] Yaochen Hu, Yushi Wang, Bang Liu, Di Niu, and Cheng Huang. Latency Reduction and Load Balancing in Coded Storage Systems. In *Proceedings of the 8th ACM Symposium on Cloud Computing (SoCC)*, 2017.

[22] Heiner Litz, Javier Gonzalez, Ana Klimovic, and Christos Kozyrakis. RAIL: Predictable, Low Tail Latency for NVMe Flash. *ACM Transactions on Storage (TOS)*, 1(1), 2021.

[23] Huaicheng Li, Mingzhe Hao, Michael Hao Tong, Swaminathan Sundararaman, Matias Bjørling, and Haryadi S. Gunawi. The CASE of FEMU: Cheap, Accurate, Scalable and Extensible Flash Emulator. In *Proceedings of the 16th USENIX Symposium on File and Storage Technologies (FAST)*, 2018.

[24] Matias Bjørling, Javier Gonzalez, and Philippe Bonnet. LightNVM: The Linux Open-Channel SSD Subsystem. In *Proceedings of the 15th USENIX Symposium on File and Storage Technologies (FAST)*, 2017.

[25] Junghee Lee, Youngjae Kim, Galen M. Shipman, Sarp Oral, Feiyi Wang, and Jongman Kim. A Semi-Preemptive Garbage Collector for Solid State Drives. In *IEEE International Symposium on Performance Analysis of Systems and Software (ISPASS)*, 2011.

[26] Pre-emptive Garbage Collection of Memory Blocks. https://www.google.com/patents/US8626986, 2014.

[27] Junghee Lee, Youngjae Kim, Galen M. Shipman, Sarp Oral, and Jongman Kim. Preemptible I/O Scheduling of Garbage Collection for Solid State Drives. In *IEEE Transactions on Computer-Aided Design of Integrated Circuits and Systems (TCAD)*, 2013.

[28] Guanying Wu and Xubin He. Reducing SSD Read Latency via NAND Flash Program and Erase Suspension. In *Proceedings of the 10th USENIX Symposium on File and Storage Technologies (FAST)*, 2012.

[29] Shine Kim, Jonghyun Bae, Hakbeom Jang, Wenjing Jin, Jeonghun Gong, Seungyeon Lee, Tae Jun Ham, and Jae W. Lee. Practical Erase Suspension for Modern Low-latency SSDs. In *Proceedings of the 2019 USENIX Annual Technical Conference (ATC)*, 2019.

[30] Erase Suspend/Resume for Memory. https://patents.google.com/patent/US9223514B2/en, 2015.

[31] John Colgrove, John D. Davis, John Hayes, Ethan L. Miller, Cary Sandvig, Russell Sears, Ari Tamches, Neil Vachharajani, and Feng Wang. Purity: Building Fast, Highly-Available Enterprise Flash Storage from Commodity Components. In *Proceedings of the 2015 ACM SIGMOD International Conference on Management of Data (SIGMOD)*, 2015.

[32] Suzhen Wu, Weidong Zhu, Guixin Liu, Hong Jiang, and Bo Mao. GC-aware Request Steering with Improved Performance and Reliability for SSD-based RAIDs. In *Proceedings of the 32th IEEE International Parallel and Distributed Processing Symposium (IPDPS)*, 2018.

[33] Youngjae Kim, Sarp Oral, Galen M. Shipman, Junghee Lee, David A. Dillow, and Feiyi Wang. Harmonia: A Globally Coordinated Garbage Collector for Arrays of Solid-state Drives. In *Proceedings of the 27th IEEE Symposium on Massive Storage Systems and Technologies (MSST)*, 2011.

[34] Jaeho Kim, Kwanghyun Lim, Youngdon Jung, Sungjin Lee, Changwoo Min, and Sam H. Noh. Alleviating Garbage Collection Interference Through Spatial Separation in All Flash Arrays. In *Proceedings of the 2019 USENIX Annual Technical Conference (ATC)*, 2019.

[35] Dimitris Skourtis, Dimitris Achlioptas, Noah Watkins, Carlos Maltzahn, and Scott Brandt. Flash on Rails: Consistent Flash Performance through Redundancy. In *Proceedings of the 2014 USENIX Annual Technical Conference (ATC)*, 2014.

[36] Jian Huang, Anirudh Badam, Laura Caulfield, Suman Nath, Sudipta Sengupta, Bikash Sharma, and Moinuddin K. Qureshi. FlashBlox: Achieving Both Performance Isolation and Uniform Lifetime for Virtualized SSDs. In *Proceedings of the 15th USENIX Symposium on*

File and Storage Technologies (FAST), 2017.

[37] Jaeho Kim, Donghee Lee, and Sam H. Noh. Towards SLO Complying SSDs Through OPS Isolation. In *Proceedings of the 13th USENIX Symposium on File and Storage Technologies (FAST)*, 2015.

[38] Mingzhe Hao, Huaicheng Li, Michael Hao Tong, Chrisma Pakha, Riza O. Suminto, Cesar A. Stuardo, Andrew A. Chien, and Haryadi S. Gunawi. MittOS: Supporting Millisecond Tail Tolerance with Fast Rejecting SLO-Aware OS Interface. In *Proceedings of the 26th ACM Symposium on Operating Systems Principles (SOSP)*, 2017.

[39] Chun-Yi Liu, Jagadish Kotra, Myoungsoo Jung, and Mahmut T. Kandemir. PEN: Design and Evaluation of Partial-Erase for 3D NAND-Based High Density SSDs. In *Proceedings of the 16th USENIX Symposium on File and Storage Technologies (FAST)*, 2018.

[40] Michael Mesnier, Jason B. Akers, Feng Chen, and Tian Luo. Differentiated Storage Services. In *Proceedings of the 23rd ACM Symposium on Operating Systems Principles (SOSP)*, 2011.

[41] George Amvrosiadis, Angela Demke Brown, and Ashvin Goel. Opportunistic storage maintenance. In *Proceedings of the 25th ACM Symposium on Operating Systems Principles (SOSP)*, 2015.

[42] Jie Zhang, Miryeong Kwon, Donghyun Gouk, Sungjoon Koh, Changlim Lee, Mohammad Alian, Myoungjun Chun, Mahmut Taylan Kandemir, Nam Sung Kim, Jihong Kim, and Myoungsoo Jung. FlashShare: Punching Through Server Storage Stack from Kernel to Firmware for Ultra-Low Latency SSDs. In *Proceedings of the 13th USENIX Symposium on Operating Systems Design and Implementation (OSDI)*, 2018.

[43] Chun-Yi Liu, Yunju Lee, Myoungsoo Jung, Mahmut Taylan Kandemir, and Wonil Choi. Prolonging 3D NAND SSD Lifetime via Read Latency Relaxation. In *Proceedings of the 26th ACM International Conference on Architectural Support for Programming Languages and Operating Systems (ASPLOS)*, 2021.

[44] Katherine Missimer and Richard West. Partitioned Real-Time NAND Flash Storage. In *Proceedings of the 39th IEEE Real-Time Systems Symposium (RTSS)*, 2018.

[45] Lalith Suresh, Marco Canini, Stefan Schmid, and Anja Feldmann. C3: Cutting Tail Latency in Cloud Data Stores via Adaptive Replica Selection. In *Proceedings of the 12th USENIX Symposium on Networked Systems Design and Implementation (NSDI)*, 2015.

[46] Zhe Wu, Curtis Yu, and Harsha V. Madhyastha. CosTLO: Cost-Effective Redundancy for Lower Latency Variance on Cloud Storage Services. In *Proceedings of the 12th USENIX Symposium on Networked Systems Design and Implementation (NSDI)*, 2015.

[47] Mingzhe Hao, Levent Toksoz, Nanqinqin Li, Edward Edberg Halim, Henry Hoffmann, and Haryadi S. Gunawi. LinnOS: Predictability on Unpredictable Flash Storage with a Light Neural Network. In *Proceedings of the 14th USENIX Symposium on Operating Systems Design and Implementation (OSDI)*, 2020.

[48] Ji-Yong Shin, Mahesh Balakrishnan, Tudor Marian, and Hakim Weatherspoon. Gecko: Contention-Oblivious Disk Arrays for Cloud Storage. In *Proceedings of the 11th USENIX Symposium on File and Storage Technologies (FAST)*, 2013.

[49] Youngjae Kim, Junghee Lee, Sarp Oral, David A. Dillow, Feiyi Wang, and Galen M. Shipman. Coordinating Garbage Collection for Arrays of Solid-State Drives. *IEEE Transactions on Computers (TC)*, 63(4), April 2014.

[50] Adrian M. Caulfield, Laura M. Grupp, and Steven Swanson. Gordon: using flash memory to build fast, power-efficient clusters for data-intensive applications. In *Proceedings of the 14th ACM International Conference on Architectural Support for Programming Languages and Operating Systems (ASPLOS)*, 2009.

[51] Feng Chen, Rubao Lee, and Xiaodong Zhang. Essential Roles of Exploiting Internal Parallelism of Flash Memory Based Solid State Drives in High-speed Data Processing. In *Proceedings of the 17th International Symposium on High Performance Computer Architecture (HPCA-17)*, 2011.

[52] Myoungsoo Jung, Wonil Choi, Miryeong Kwon, Shekhar Srikantaiah, Joonhyuk Yoo, and Mahmut Kandemir. Design of a Host Interface Logic for GC-Free SSDs. *IEEE Transactions on Computer-Aided Design of Integrated Circuits and Systems (TCAD)*, 8(1), May 2019.

[53] Ana Klimovic, Heiner Litz, and Christos Kozyrakis. ReFlex: Remote Flash ≈ Local Flash. In *Proceedings of the 22nd ACM International Conference on Architectural Support for Programming Languages and Operating Systems (ASPLOS)*, 2017.

[54] Tianyang Jiang, Guangyan Zhang, Zican Huang, Xiaosong Ma, Junyu Wei, Zhiyue Li, and Weimin Zheng. FusionRAID: Achieving Consistent Low Latency for Commodity SSD Arrays. In *Proceedings of the 19th USENIX Symposium on File and Storage Technologies (FAST)*, 2021.

[55] Sudharsan Seshadri, Mark Gahagan, Sundaram Bhaskaran, Trevor Bunker, Arup De, Yanqin Jin, Yang Liu, and Steven Swanson. Willow: A User-Programmable SSD. In *Proceedings of the 11th USENIX Symposium on Operating Systems Design and Implementation (OSDI)*, 2014.

[56] Sungjin Lee, Ming Liu, SangWoo Jun, Shuotao Xu, Jihong Kim, and Arvind. Application-Managed Flash. In *Proceedings of the 14th USENIX Symposium on File and Storage Technologies (FAST)*, 2016.

[57] Yiying Zhang, Leo Prasath Arulraj, Andrea C. Arpaci-Dusseau, and Remzi H. Arpaci-Dusseau. De-indirection for Flash-based SSDs with Nameless Writes. In *Proceedings of the 10th USENIX Symposium on File and Storage Technologies (FAST)*, 2012.

[58] Matias Bjørling, Abutalib Aghayev, Hans Holmberg, Aravind Ramesh, Damien Le Moal, Greg R. Ganger, and George Amvrosiadis. ZNS: Avoiding the Block Interface Tax for Flash-based SSDs. In *Proceedings of the 2021 USENIX Annual Technical Conference (ATC)*, 2021.

[59] Amy Tai, Igor Smolyar, Michael Wei, and Dan Tsafrir. Optimizing Storage Performance with Calibrated Interrupts. In *Proceedings of the 15th USENIX Symposium on Operating Systems Design and Implementation (OSDI)*, 2021.

[60] Miryeong Kwon, Donghyun Gouk, Changrim Lee, Byounggeun Kim, Jooyoung Hwang, and Myoungsoo Jung. DC-Store: Eliminating Noisy Neighbor Containers using Deterministic I/O Performance and Resource Isolation. In *Proceedings of the 18th USENIX Symposium on File and Storage Technologies (FAST)*, 2020.

[61] Redundant Array of Independent NAND for a Three-dimensional Memory Array. https://patents.google.com/patent/US20170249211A1/en, 2019.

[62] Martin Maas, Krste Asanovic, Tim Harris, and John Kubiatowicz. Taurus: A Holistic Language Runtime System for Coordinating Distributed Managed-Language Applications. In *Proceedings of the 21st ACM International Conference on Architectural Support for Programming Languages and Operating Systems (ASPLOS)*, 2016.

[63] Martin Maas, Tim Harris, Krste Asanovic, and John Kubiatowicz. Trash Day: Coordinating Garbage Collection in Distributed Systems. In *Proceedings of the 15th Workshop on Hot Topics in Operating Systems (HotOS XV)*, 2015.

[64] Joonsung Kim, Pyeongsu Park, Jaehyung Ahn, Jihun Kim, Jong Kim, and Jangwoo Kim. SSDcheck: Timely and Accurate Prediction of Irregular Behaviors in Black-Box SSDs. In *51st Annual IEEE/ACM International Symposium on Microarchitecture (MICRO-51)*, 2018.

[65] What's the State of DWPD? Endurance in Industry Leading Enterprise SSDs. http://www.storagesearch.com/dwpd.html, 2020.

[66] Speeds, Feeds and Needs – Understanding SSD Endurance. https://blog.westerndigital.com/ssd-endurance-speeds-feeds-needs/, 2015.

[67] Non-Volatile Random-Access Memory. https://en.wikipedia.org/wiki/Non-volatile_random-access_memory, 2021.

[68] Intel Optane Persistent Memory (PMem). https://www.intel.com/content/www/us/en/architecture-and-

technology/optane-dc-persistent-memory.html, 2021.

[69] IODA Github Homepage. https://github.com/huaicheng/IODA, 2021.

[70] FEMU Github Homepage. https://github.com/ucare-uchicago/femu, 2018.

[71] Yun-Sheng Chang, Yao Hsiao, Tzu-Chi Lin, Che-Wei Tsao, Chun-Feng Wu, Yuan-Hao Chang, Hsiang-Shang Ko, and Yu-Fang Chen. Determinizing Crash Behavior with a Verified Snapshot-Consistent Flash Translation Layer. In *Proceedings of the 14th USENIX Symposium on Operating Systems Design and Implementation (OSDI)*, 2020.

[72] Huaicheng Li, Mingzhe Hao, Stanko Novakovic, Vaibhav Gogte, Sriram Govindan, Dan R. K. Ports, Irene Zhang, Ricardo Bianchini, Haryadi S. Gunawi, and Anirudh Badam. LeapIO: Efficient and Portable Virtual NVMe Storage on ARM SoCs. In *Proceedings of the 25th ACM International Conference on Architectural Support for Programming Languages and Operating Systems (ASPLOS)*, 2020.

[73] Open-Channel Solid State Drives. http://lightnvm.io/.

[74] Emulab D430s. https://gitlab.flux.utah.edu/emulab-devel/wikis/Utah-Cluster/d430s, 2017.

[75] Ultra-Low Latency with Samsung Z-NAND SSD. https://www.samsung.com/us/labs/pdfs/collateral/Samsung_Z-NAND_Technology_Brief_v5.pdf, 2020.

[76] SNIA I/O Trace Data Files. http://iotta.snia.org/traces, 2016.

[77] Filebench. https://github.com/filebench/filebench/wiki.

[78] Brian F. Cooper, Adam Silberstein, Erwin Tam, Raghu Ramakrishnan, and Russell Sears. Benchmarking Cloud Serving Systems with YCSB. In *Proceedings of the 1st ACM Symposium on Cloud Computing (SoCC)*, 2010.

[79] Sysbench. https://github.com/akopytov/sysbench, 2020.

[80] HiBench: The Bigdata Micro Benchmark Suite. https://github.com/Intel-bigdata/HiBench, 2020.

[81] Ganesh Ananthanarayanan, Ali Ghodsi, Scott Shenker, and Ion Stoica. Effective Straggler Mitigation: Attack of the Clones. In *Proceedings of the 10th USENIX Symposium on Networked Systems Design and Implementation (NSDI)*, 2013.

[82] Myungsuk Kim, Jisung Park, Geonhee Cho, and Yoona Kim. Evanesco: Architectural Support for Efficient Data Sanitization in Modern Flash-Based Storage Systems. In *Proceedings of the 25th ACM International Conference on Architectural Support for Programming Languages and Operating Systems (ASPLOS)*, 2020.

[83] Yang Hu, Hong Jiang, Dan Feng, Lei Tian, Hao Luo, and Shuping Zhang. Performance Impact and Interplay of SSD Parallelism through Advanced Commands, Allocation Strategy and Data Granularity. In *Proceedings of the 25th International Conference on Supercomputing (ICS)*, 2011.